BOLETÍN GEOLÓGICO Y MINERO 136 (2)
abril-junio 2025, 006
ISSN-L: 0366-0176, eISSN: 2253-6167
https://doi.org/10.21701/bolgeomin/136.2/006

Boletín
Geológico y
Minero

RESEARCH ARTICLE

Portable X-Ray Fluorescence and Gamma Ray Spectrometry exploration in the Serra da Neve Alkaline Complex, SW Angola

Prospección con Fluorescencia Rayos X y Espectrómetro Rayos Gama portable en el Complexo Alcalino de Serra da Neve, SW Angola

Cátia Prazeres[(1)]*, **Maria João Batista**[(1)], **Rui Lopes**[(2)], **Bruno Barros**[(2)], **José Labaredas**[(2)], **José Feliciano Rodrigues**[(1)], **Domingos Cordeiro**[(3)]

[(1)] *Laboratório Nacional de Energia e Geologia (LNEG), Estrada da Portela, Bairro do Zambujal, 2610-999 Amadora, Portugal*
[(2)] *UTE-PLANAGEO (IGME/LNEG/Impulso), Parque tecnológico de Asturias, parcela 13 A, 33428, Asturias, España*
[(3)] *Instituto Geológico de Angola (IGEO), Centralidade do Kilamba, Luanda, Angola*

***Corresponding author:** catia.prazeres@lneg.pt (Cátia Prazeres)

Key points:

Field exploration techniques were used in SW Angola during the PLANAGEO project including pXRF and pGRS in the SNAC for the first time.

Geochemical affinities are taken advantage of for exploration in alkaline rocks, where U and Th can be used as pathfinders for REE and guide field work.

REE distribution in the SNAC is biased by the SE anomaly in the Nejoio satellite intrusion.

ABSTRACT

During PLANAGEO project, some areas were selected to undergo exploration programs according to target materials – Au (Fe); REE (Nb-Ta); Ni/Cr/Pt - using handheld field instruments. Portable instruments are widely used in exploration as a prompt way of obtaining information and direct field work and subsequent investigations. The Serra da Neve Alkaline Complex (SNAC) is a wide set of volcanic and subvolcanic structures that host REE (Nb-Ta)-bearing mineralogy. The same potential exists for elements with similar geochemical behavior such as incompatible trace elements, Large-Ion Lithophile Elements (LILE) and High-Field Strength Elements (HFSE), such as U and Th. The survey for a group of elements obtained by X-Ray Fluorescence and for equivalent Uranium (eU), equivalent Thorium (eTh) and Potassium by Gamma Ray Spectrometry showed similarities in their concentrations in rock sample sites. U and especially Th distribution show the same patterns as REE in different lithologies within the SNAC, mainly in the syenites. Nb tends to concentrate in alkaline dikes, apart from ijolites. There is a clear anomaly to be followed in the SE zone, in the Nejoio satellite intrusion.

Article History:
Received: 05/02/2024
Accepted: 05/03/2025
Published: 10/04/2026

Keywords: Serra da Neve; portable instruments; REE (Nb-Ta); alkaline rocks

Puntos clave:

Las técnicas de exploración de campo utilizadas en el SO de Angola durante el proyecto PLANAGEO incluirán FRXp y GRSp por la primera vez en el SNAC.

Las afinidades geoquímicas se aprovechan para la exploración en rocas alcalinas, donde U y Th pueden usarse como indicadores para REE y guiar el trabajo de campo.

La distribución de REE en el Complejo Alcalino de Serra da Neve está sesgada por la anomalía SE en la intrusión satélite de Nejoio.

RESUMEN

Durante el proyecto PLANAGEO, se seleccionaron algunas áreas para someterlas a programas de exploración según los materiales objetivo – Au (Fe); REE (Nb-Ta); Ni/Cr/Pt - mediante el uso de instrumentos de campo portátiles. Estos instrumentos portátiles se utilizan ampliamente en la prospección como una forma rápida de obtener información y orientar el trabajo de campo y las investigaciones posteriores. El Complejo Alcalino de Serra da Neve (SNAC) es un amplio conjunto de estructuras volcánicas y subvolcánicas que albergan mineralogía portadora de ETR (Nb-Ta). El mismo potencial existe para elementos con comportamiento geoquímico similar, como elementos incompatibles, elementos litófilos de grandes radios iónicos (LILE) y elementos de alta fuerza de campo (HSFE), como U y Th. El estudio de un grupo de elementos obtenidos mediante fluorescencia de rayos X y de Uranio equivalente (eU), Torio equivalente (eTh) y Potasio mediante espectrometría de rayos gamma mostró similitudes en los puntos de muestreo de rocas. La distribución de U y especialmente de Th muestran los mismos patrones que las tierras raras en diferentes litologías dentro del SNAC, principalmente en las sienitas. El Nb tiende a concentrarse en diques alcalinos, aparte de en las ijolitas. Una clara anomalía que seguir es la zona SE, en la intrusión satélite de Nejoio.

Historial del artículo:
Received: 05/02/2024
Accepted: 05/03/2025
Published: 10/04/2026

Palabras clave: Serra da Neve; instrumentos portables; ETR (Nb-Ta); rocas alcalinas

Citation / Cómo citar este artículo: Prazeres, C., Batista, M.J., Lopes, R., Barros, B., Labaredas, J., Rodrigues, J.F., Cordeiro, D. (2025). Portable X-Ray Fluorescence and Gamma Ray Spectrometry exploration in the Serra da Neve Alkaline Complex, SW Angola. Boletín Geológico y Minero, 136(2), 006. http://dx.doi.org/10.21701/bolgeomin/136.2/006

1. Introduction

Within the scope of the PLANAGEO project – Angolan National Program of Geology, the consortium formed by the Geological Surveys of Spain and Portugal - UTE (IGME-LNEG) was responsible for the cartography of the SW of the country. A subproject was designed for Metallic Mineral Resources Mapping (CRMMA). Work areas, or clusters, were chosen according to target raw materials potential. This way, one cluster was targeting Au (Fe), another targeting REE (Nb-Ta), and a third one aiming for Ni-Cr-Pt. Therefore, each area had its proper exploration strategy and field surveys delineated. In this framework, the Serra da Neve Alkaline Complex (SNAC) was studied for its potential on REE (Nb-Ta). This complex is a large set of volcanic, subvolcanic and plutonic alkaline rocks, with little work done in exploration.

Characterization and exploration of an area is a multidisciplinary and multiscale activity and much of the research on carbonatites and alkaline bodies for REE exploration has been made by geological survey and geochemical or geophysical pathfinder signatures (Banks et al., 2019). Therefore, apart from the direct measurement of the target element, data on alteration patterns or indicator elements or minerals is used to provide information on the source conditions that lead to the target. Moreover, field analytical techniques have improved greatly in the last few years and allow for high density, cost-effective surveys to better guide campaigns and help to make decisions.

The group of metals referred to as rare earth elements (REE) comprises the 15 elements of the lanthanide series and yttrium (Y), that shares similar geochemical behavior, for its similar chemical and physical properties. Yttrium has an ionic radius nearly identical to that of holmium (Ho) and thus is commonly included with Heavy Rare Earth Elements (HREE) (e.g. Bau and Dulsky, 1996). Niobium shares many of its properties with tantalum, which it is commonly found with, and it is explored along with REE and Zr. In fact, Nb is present in igneous rocks, mainly in alkaline types in Zr or Ti minerals.

Felsic igneous rocks are often enriched in these elements that are concentrated in the residual melt during the later stages of fractional crystallization. Furthermore, alkaline, peralkaline granites, carbonatites, peraluminous granites and pegmatites usually host accessory mineralogy that bear Large Ion Lithophile Elements (LILE) and High-Field Strength Elements (HFSE), including K, U and Th (e.g. Shives, 2015).

In this case, elemental concentrations were assessed in the SNAC and surrounding rocks, through portable X-ray fluorescence and a portable gamma-ray spectrometer was used at the same locations for a regional survey. Information is mapped and compared, and preferential zones are defined.

2. Geological setting

The SNAC constitutes a set of interconnected elliptic and round volcanic and subvolcanic rock bodies aligned in an overall WNW-ESE trend (Fig. 1). Emplacement of the alkaline shallow intrusions took place during middle to upper Cretaceous intruding and fenitizing Eburnean granitic and migmatitic rocks from the Angolan shield. The NW-SE to WNW-ESE trend is a transverse direction to the main Transangolan Belt orientation. This alignment (NE-SW trend) crosses the country and is part of the Paraná-Angola-Namibia tectonic alignment (e.g. Comin-Chiaramonti et al., 2007) that hosts several kimberlitic and carbonatitic structures (Rodrigues, 1972). The SNAC set of volcanic-subvolcanic bodies is crossed by a set of dike swarms that follow different trends associated with the implementation of the complex, but also apparently emplaced through fractures with the same structural trend as NW-SE Mesoproterozoic dike swarms.

Pereira and Moreira (1978) showed that the emplacement of the SNAC followed a SE to NW trend, from the more undersaturated magmatic terms to the more supersaturated ones. The eastern structure is the Nejoio satellite body, composed of nepheline syenites and an ijolitic outer ring. Most of it is surrounded by fenitization aureole. The intrusive terms are composed of alkaline and peralkaline granites, syenites, nepheline-syenite porphyries and ijolites. Many of the alkaline rocks developed fenites as a result of metasomatism in the contact with the Paleoproterozoic granitic-migmatitic surrounding rocks (Rodrigues, 1973).

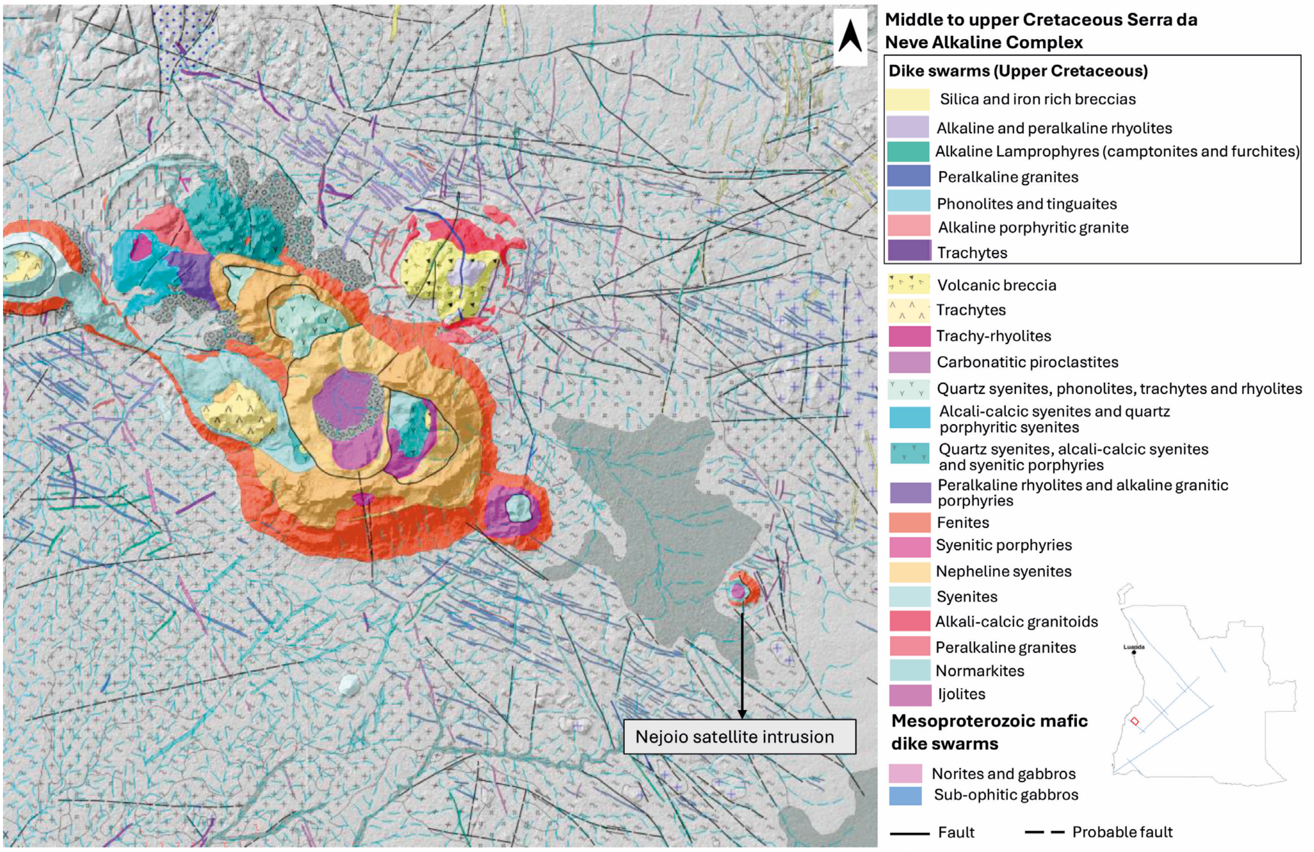

Figure 1. Geological map of the SNAC within the frame of the working area, from Lopes and Caessa (2021). Geological legend is simplified. Units in light grey are Eburnean age metamorphic and igneous rocks; units in dark grey are recent, superficial deposits.

Figura 1. Mapa geológico de la SNAC inserido en el área de trabajo, modificado de Lopes *and* Caessa (2021). La leyenda geológica está simplificada. Las unidades en gris claro son rocas ígneas y metamórficas eburneanas; las unidades en gris oscuro son depósitos superficiales recientes.

Alkali-calcic syenites in the SNAC contain alkali feldspar, pyroxene and accessory sphene, apatite, zircon and carbonates. Nordmarkite type syenites (with quartz in variable amounts) on the NW portion comprise hornblende, augite, iron oxides, apatite, biotite, aegirine, fluorite, riebeckite, titanite and rarely arfvedsonite as accessory minerals (Pereira and Moreira, 1978). Ijolitic composition is sometimes represented (Lopes and Caessa, 2021). In these rocks, essential mineralogy is mainly felsic, nepheline and cancrinite are frequent, but aegirine, biotite and kaersutite were also identified. Apatite and carbonate are also present as accessories.

The bodies that constitute the SNAC display, in general, a volcanic and sub-volcanic center, constituted mainly by volcanic breccias, basalts, trachytes, phonolites, carbonatitic pyroclasts, besides syenitic to quartz-syenitic porphyries (Pereira and Moreira, 1978; Lopes and Caessa, 2021). Volcanic breccias agglomerate trachytic lavas and fragments of other rocks, including syenites. Trachytes themselves show a main composition of sanidine, albite and some anorthoclase, with iron oxides and sometimes carbonates and quartz (Pereira and Moreira, 1978).

3. Methodology

Portable analytical instruments enabled a larger scale coverage and enhanced observational resolution for exploration. This 1:100000 sheet (295-Capira), corresponding to a nearly 3000 Km^2 area was subjected to a field survey designed to characterize and find anomalies that could conduct further exploration targets for REE. A total of 287 measurements were taken, in the same sites, with both portable X Ray Fluorescence (pXRF) and portable Gamma Ray Spectrometer (pGRS) on a nonregular grid, due to difficult access of the region. Rocks, stream sediments and soils were subjected to readings. In total, 135 rock samples, 127 stream sediments and 25 soils were evaluated, although soil samples are not considered in this study due to the small number of measurements and thus lack of statistical significance. Rock samples were preferably analyzed in the area occupied by the SNAC, trying to contemplate as much lithologies as the accessibility would allow, and sediment samples were favored in the surrounding area, towards which the flow of the washed materials would run off. This type of sample would possibly contain weathering resistant species, as is the case for many REE-bearing minerals.

After the acquisition of radiometric data and in situ chemical analysis, the dataset was subjected to univariate statistical analysis to validate it and proceed for the generation of maps that reflect data distribution. From the statistical analysis, percentiles were calculated as a criterion of class grouping to display on map, to better show the higher concentration areas. Only classes corresponding to percentiles greater than 75% were further grouped and considered to define associations to the lithology.

3.1. Portable XRF

Portable XRF (pXRF) was used throughout the regions studied in PLANAGEO. An EDXRF Hitachi/X-MET800 model, with a 45kV X-ray tube, 25 mm^2 detection area was employed. Presently, pXRF is used broadly in mineral exploration for being a cost-effective instrument to guide operations (e.g. Fisher, 2014). In fact, it can provide on-site chemical analysis of over 30 elements. XRF analysis is based on the amount of energy, specific to each element, that is necessary to induce electron transitions between layers of the atom, once a sample is irradiated with X-rays. As those transitions are accompanied by photon emissions, with characteristic energies, this allows the identification of the atomic species and the chemical element, as well as its concentration, from the intensity of the energy detected.

This technique presents, however, some limitations in its use on the field, namely the high detection limits, beam dispersion, especially when analyzing irregular samples, or the effect of grain size (e.g., Ravansari, 2019). In order to control the confidence level of the results, calibration was verified daily with the use of certified reference materials. Measurements were taken directly on the sample during 120 s applying normal calibration (MINING-LE-FP) and REE calibration using a collimator (3mm diameter analysis spot), as a compromise for time consumed and thoroughness in each site. Three readings were performed in each outcrop to avoid nugget effect.

The elements considered in the pXRF survey were La (ppm), Y (ppm) and Nb (ppm). This selection reflects global significance of measurements, meaning elements whose concentrations were consistently read by the equipment along with the affinity of this group of elements in such geological environment and association to the target material.

3.2. Portable GRS

Simultaneously to portable XRF, in the work areas dedicated to REE exploration, a portable Gamma Ray Spectrometer (pGRS) was used, in this case, a GT-32 GEORADIS model, with a BGO detector 2x2”. GRS provides concentrations of K (%), eU (ppm) and eTh (ppm), for these elements have naturally occurring radioactive isotopes that produce gamma rays of sufficient energy and intensity to be measured by gamma ray spectrometry, which are ^{40}K (K), ^{214}Bi (U) and ^{208}Tl (Th) (IAEA, 2003). Due to the aforementioned geochemical affinity, GRS is commonly used as a primary exploration tool for REE. Readings were performed on the samples for 120 s. The geometry of the measured spot is important, where the more planar the better. In the same way as for pXRF, measurements are taken in direct contact with the surface of the rock or sediment, without any vegetable cover, and on the same sites.

4. Results

4.1. pXRF – distribution of La, Y and Nb

Points where data was too low to be recorded were assigned with half of the minimum value detected for that element, for statistical calculations. Table 1 displays the univariate statistics for all selected elements. The effect of extreme values is noticeable from the measures of dispersion, meaning elements of interest concentrate in certain zones of the working area and are not evenly distributed.

Rock sampling points									
	Min	**Max**	**Varia**	**StandDev**	**AritMeam**	**GeoMean**	**Median**	**Mode**	**n**
La *ppm*	3.500	24646.000	4440392.791	2107.224	265.404	55.789	67.000	3.500	135
Y *ppm*	1.000	582.000	2796.055	52.878	34.452	22.795	25.000	35.000	135
Nb *ppm*	0.500	776.000	25102.560	158.438	146.619	59.603	111.000	0.500	135
Stream sediment sampling points									
	Min	**Max**	**Varia**	**StandDev**	**AritMeam**	**GeoMean**	**Median**	**Mode**	**n**
La *ppm*	2.500	183.000	1148.512	33.890	18.043	5.226	2.500	2.500	127
Y *ppm*	0.500	101.000	125.152	11.187	7.819	5.548	5.000	5.000	127
Nb *ppm*	0.500	678.000	5839.832	76.419	21.134	3.635	6.000	0.500	127

Table 1. Univariate statistics for the data obtained by pXRF for elements of interest.

Tabla 1. Estadística univariada para los datos obtenidos por pXRF para los elementos de interés.

Selected elements analyzed by pXRF are overall more concentrated in the SNAC rather than in the surrounding, older terrain, for both sampling media, and in certain preferential directions, WNW-ESE and NE-SW, those of the SNAC. Excepting niobium, more dispersed in the study area (Fig. 2 and 3). The maximum values recorded for the REE are associated with the Nejoio satellite body, showing exceptionally high concentrations, that are outlying from the average of the region.

Lanthanum is one of the most abundant REE, together with Ce, Y and Nd (Chakhmouradian and Wall, 2012). In this work, concentrations reach more than 20000 ppm in the outstanding rock sample site from Nejoio, but nevertheless, values in the order of 400 ppm occur in nepheline syenites and ijolites within the SNAC. Stream sediments, however, show in general, lower concentrations.

The distribution pattern of yttrium in this area is identical to that of La for rock samples, showing an extreme concentration value of 1565 ppm in Nejoio, that has no equivalent in any other measured point. Stream sediments map (Fig.3) shows both La and Y are rather restricted to the SNAC area, although La concentrations are also higher in W-E faults in the south and in the NE zone, even though concentration values do not go above 200 ppm.

The more substantial concentrations of Nb are found in ijolites and syenitic porphyries inside the SNAC and, differently from the formerly described, La-Y concentration distributions, also associated to NE-SW alkaline dike swarms, south from the SNAC, and not presenting an outlier maximum value. Concentrations reach near 800 ppm. For stream sediments samples, Nb tends to concentrate in the ijolites but also in the diatexites zones, probably through dispersion and flow through fractures (Fig. 3).

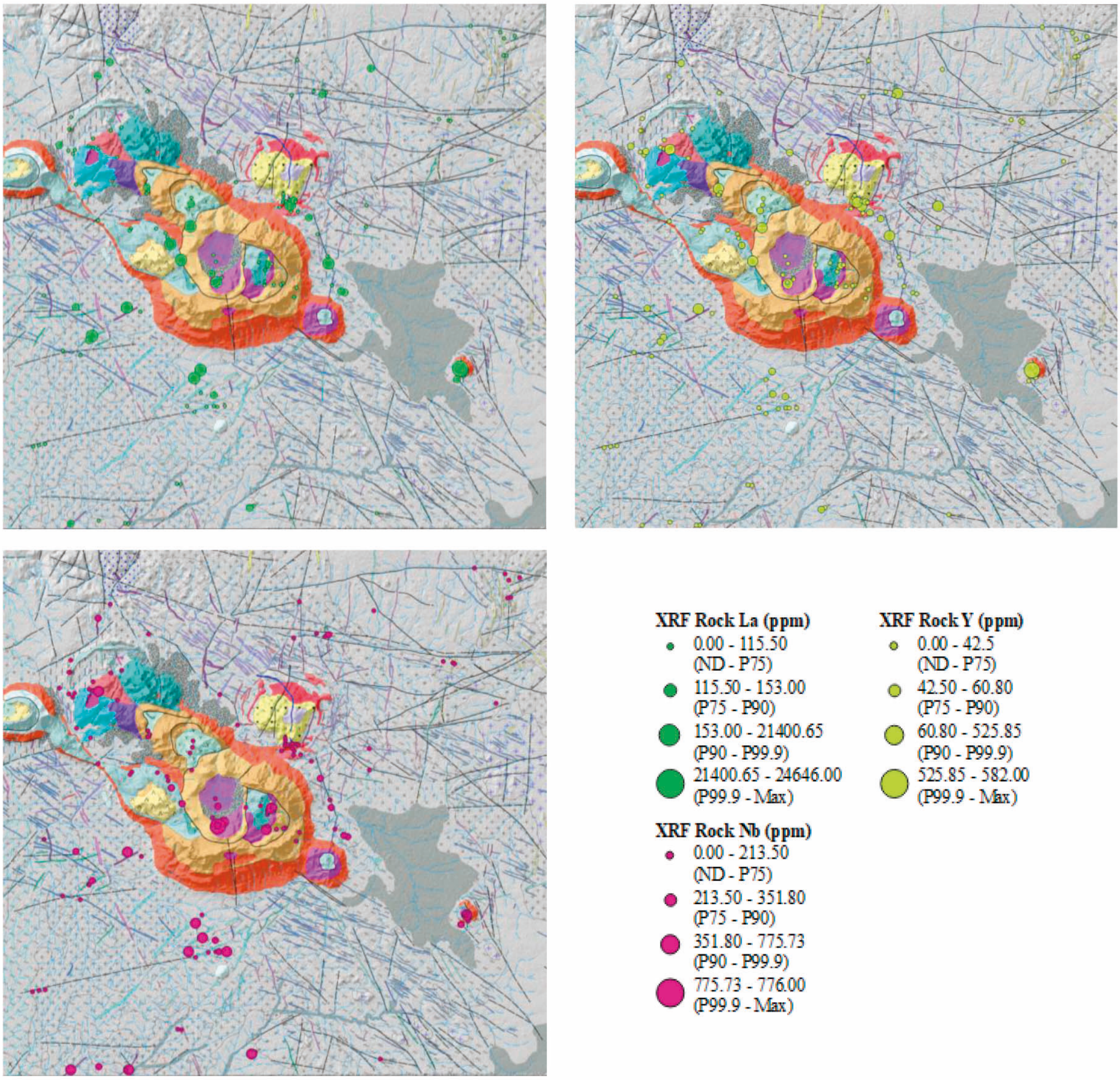

Figure 2. Distribution maps of La, Y and Nb concentrations in rocks, measured by pXRF. Percentile classes in brackets; ND: not detected.

Figura 2. Mapas de distribución de la concentración de La, Y y Nb en rocas, medido por pXRF. Clases de percentiles entre paréntesis; ND: no detectado.

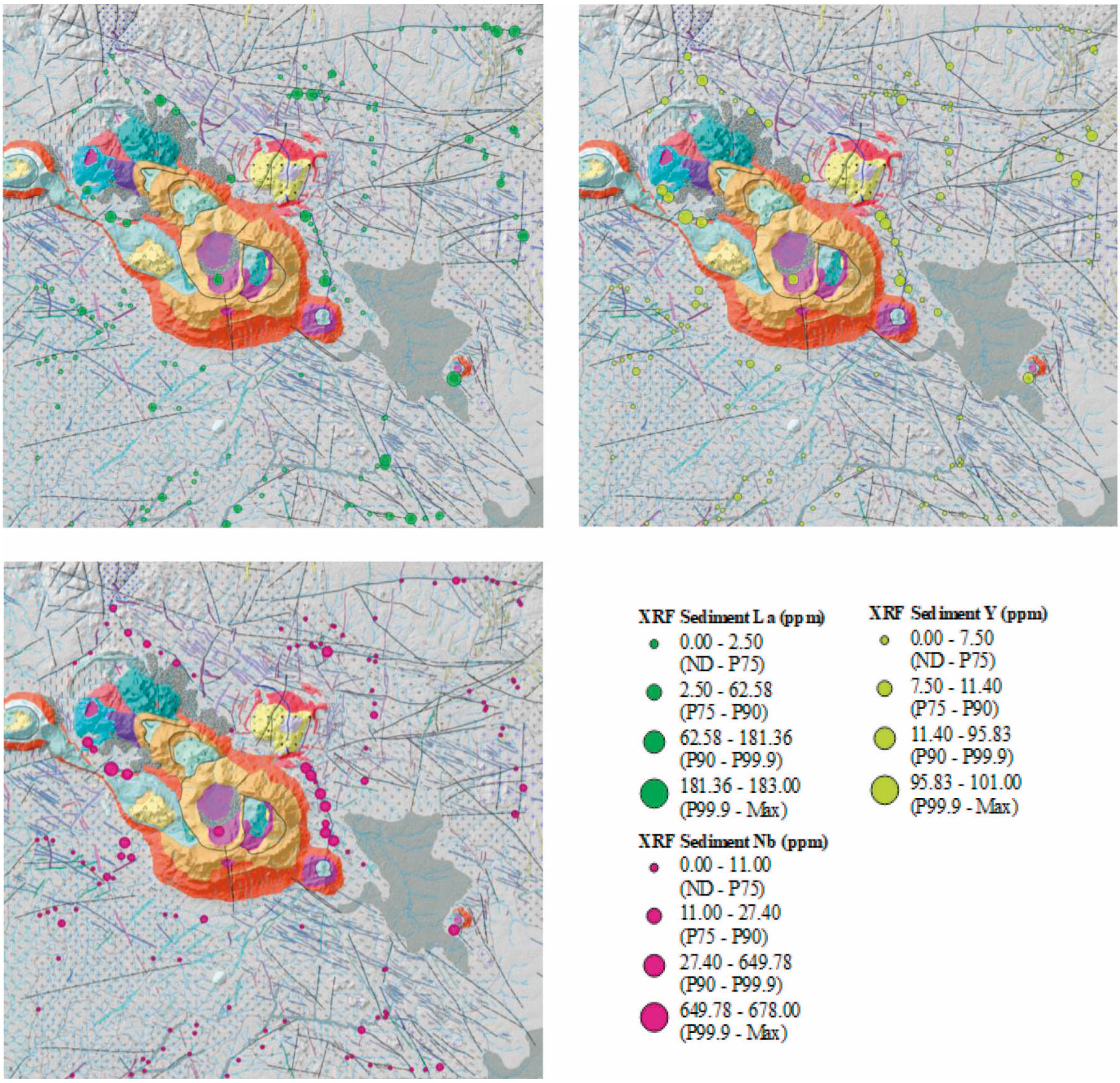

Figure 3. Distribution maps of La, Y and Nb concentrations in stream sediments, measured by pXRF. Percentile classes in brackets; ND: not detected.

Figura 3. Mapas de distribución de la concentración La, Y y Nb en sedimentos de corriente, medidos por pXRF. Clases de percentiles entre paréntesis; ND: no detectado.

4.2. pGRS - distribution of eU, eTh, K

The results for uranium and thorium concentration in rocks are overshadowed by the sampling point in the Nejoio body, with much higher concentration than the rest of the sites, which is a setting to be further studied. Statistics of this distribution are shown in table 2.

Rock sampling points									
	Min	**Max**	**Varia**	**StandDev**	**AritMeam**	**GeoMean**	**Median**	**Mode**	**n**
Total *cps*	4.455	2767.412	55156.625	234.854	87.442	59.808	56.908	53.897	135
K *%*	0.3	8.3	1.982	1.408	3.95	3.594	4.2	4	135
eU *ppm*	0	94.4	89.568	9.464	6.81	–	4.6	4.2	135
eTh *ppm*	1.4	2441.9	43403.435	208.335	46.427	22.731	21.2	18.8	135
eU/eTh	0	0.678	0.012	0.111	0.225	–	0.221	0.257	135
Stream sediment sampling points									
	Min	**Max**	**Varia**	**StandDev**	**AritMeam**	**GeoMean**	**Median**	**Mode**	**n**
Total *cps*	19.91	134.122	336.007	18.33	36.293	33.769	31.592	32.81	127
K *%*	1.8	5.5	0.494	0.703	3.506	3.433	3.5	3.5	127
eU *ppm*	0	11.4	2.954	1.719	1.732	–	1.3	1.8	127
eTh *ppm*	2.9	92.9	163.464	12.785	11.291	8.697	7.9	9.5	127
eU/eTh	0	0.483	0.011	0.106	0.175	–	0.164	0.173	127

Table 2. Univariate statistics for the data obtained by pGRS.

Tabla 2. Estadística univariada para los datos obtenidos por pGRS.

Th is especially concentrated in the Nejoio rock sample, indicating 2441 ppm eTh, while all other measuring points are below 500 ppm (Fig. 4). Th is always higher than U, for all samples, which is expressed by the consistently low U/Th ratios (Table 2). In this study, uranium and thorium distribution in stream sediments do not differ greatly from each other (Fig. 5). Higher concentrations are observed in the Nejoio area, but also occur in W-E fault zones, or in a silica/iron-rich breccia vein zone in the NE of the map area. Closer to the SNAC, higher concentration follow the NW-SE trend of the complex itself. Nevertheless, measured concentrations are lower than for rock samples, never surpassing 93 ppm for eTh and 11 ppm for eU.

Potassium maps reveal widespread concentration values across the study area in both rock and sediment sites. However, the rock samples particularly highlight the SNAC area, with the highest concentration observed in Nejoio, reaching 8.3%. Sediment measurement points where concentrations are higher show some association in the south part of the map to larger accumulation zones of the drainage network. Concentration values go to a maximum of 5.5 % in these samples.

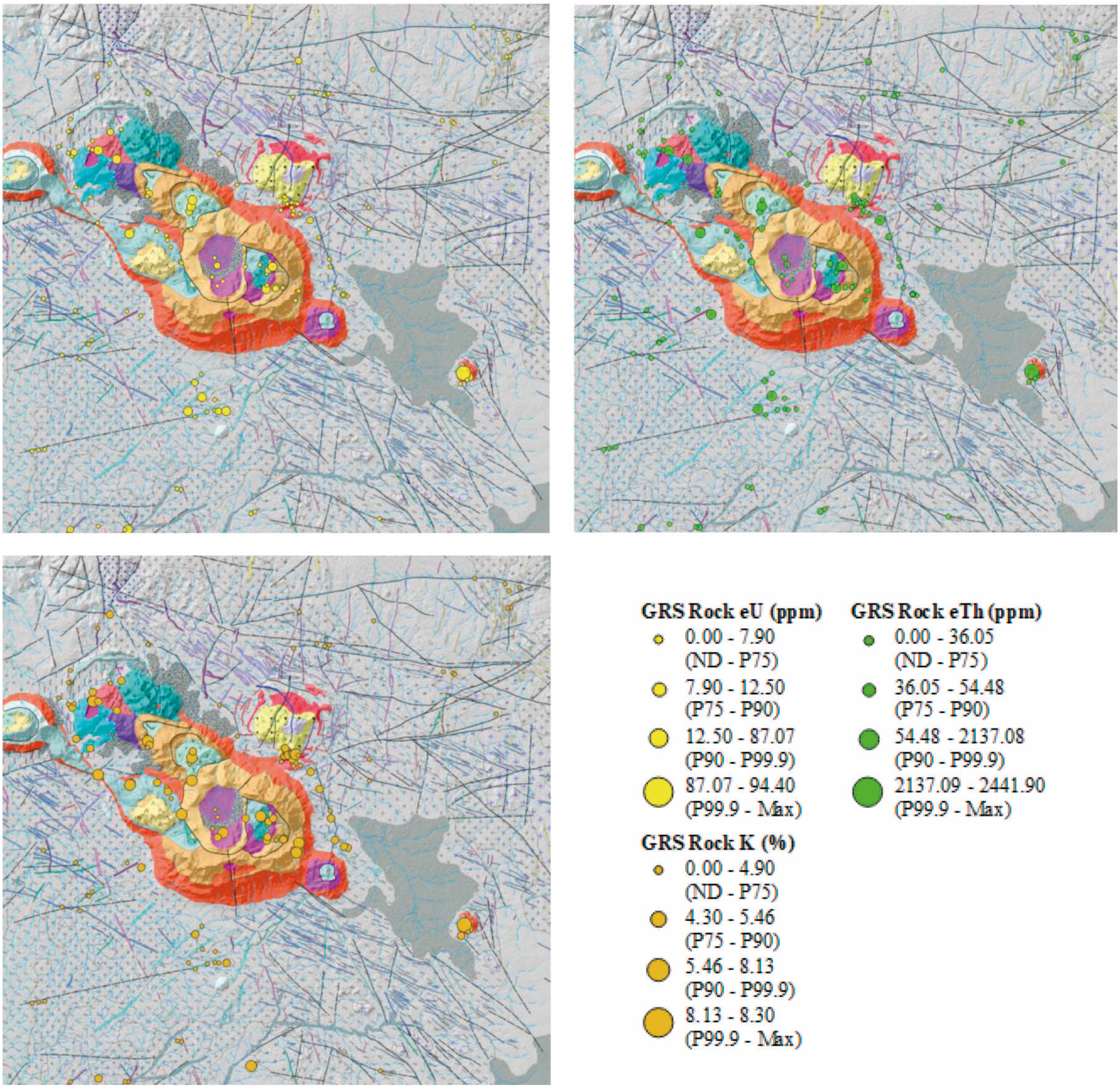

Figure 4. Distribution maps of eU, eTh and K in rocks, measured by pGRS. Percentile classes in brackets; ND: not detected.

Figura 4. Mapas de distribución de eU, eTh y K en rocas, medido por pGRS. Clases de percentiles entre paréntesis; ND: no detectado.

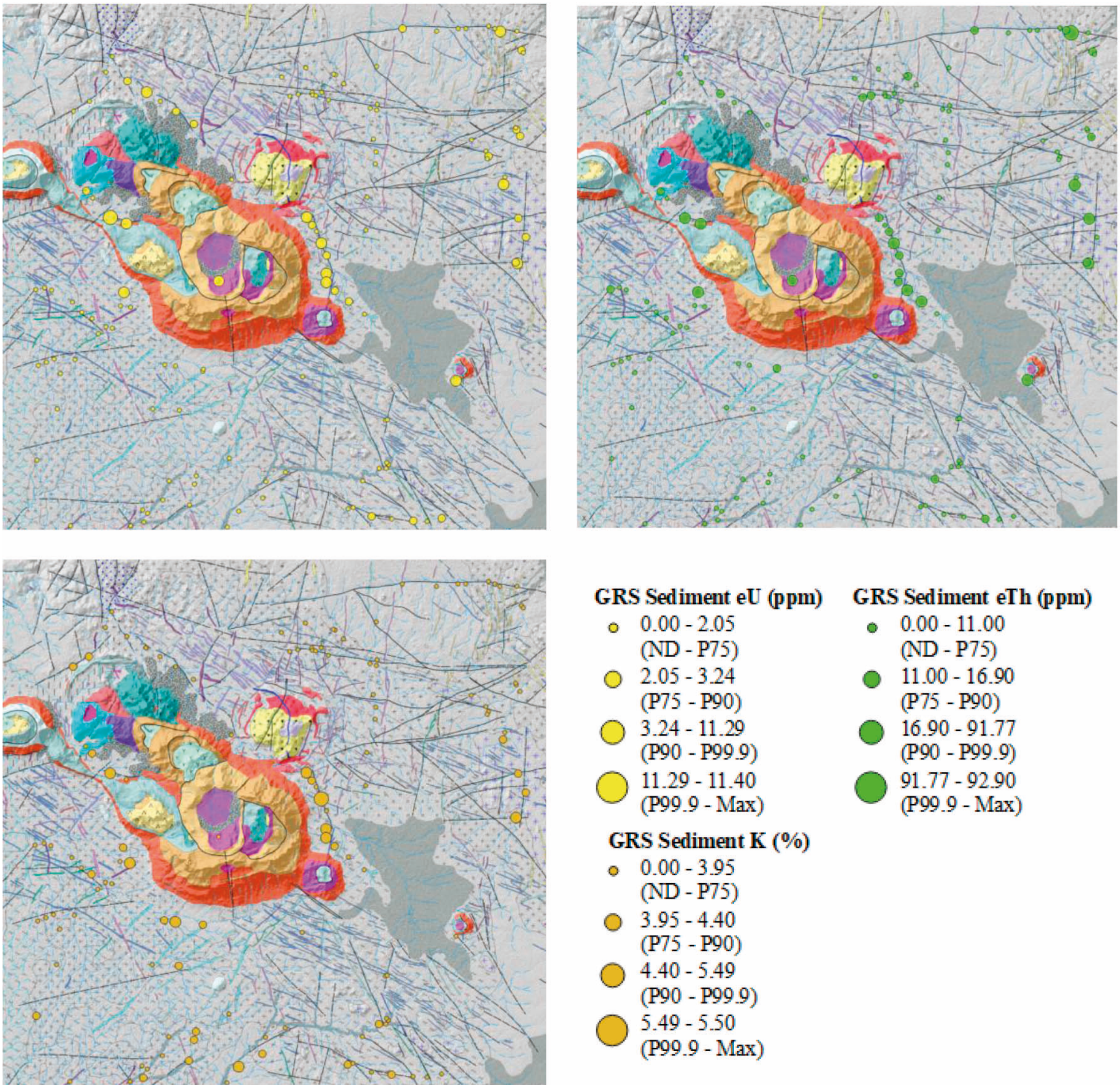

Figure 5. Distribution maps of eU, eTh and K in stream sediments, measured by pGRS. Percentile classes in brackets; ND: not detected.

Figura 5. Mapas de distribución de eU, eTh y K en sedimentos de corriente, medido por pGRS. Clases de percentiles entre paréntesis; ND: no detectado.

5. Discussion

It has been shown that concentrations of elements of interest in the SNAC intrusions stand out from the host rocks, for its composition is very different from the one of the Angolan shield basement rocks, that is intruded. Nevertheless, some of the measured values are in fact considerable, adding to the notable influence of the Nejoio intrusion and the contribution of syenitic and ijolitic lithologies and faults and alkaline veins.

Lanthanum and yttrium were measured consistently during the field work and represent the presence of REE. Both elements show a similar behavior in rock samples, comparable to that of thorium in pGRS, meaning it is dominated by the Nejoio intrusion. The Nejoio extreme values can be explained by the existence of an outcrop, within the outer ring syenites, not mappable at this scale, that contains bastnasite (Ce) - $Ce(CO_3)F$ (Prazeres et al., 2023). Bastnasite also usually hosts U and Th (Zhu, 2015) and thus is responsible for these values. Nonetheless, other works have mentioned the presence of pyrochlore in this body (Borst, 2021). However, the presence of REE in the remaining intrusive bodies of the SNAC must be related to other REE-carrying mineralogy, such as sphene, apatite, or eudialyte, that have been described by Pereira (1978).

Although U is more mobile than Th in oxidizing conditions, both seem very restricted to the SNAC and fault zones. Thorium tends to stay in its Th^{4+} form and has a more immobile behavior. The main differences between uranium and thorium radioelements mobilization comprise the uranium leaching capacity and thorium immobilization on organic and inorganic pedogenic substances (Moyen et al., 2021). The U^{4+} ion is essentially insoluble, but uranium mobilization occurs due to weathering and its solubilization is significantly increased in oxidizing environments due to the formation of the hexavalent (U^{6+}) uranyl ion (UO_2^{2+}) (Murakami, 1997). However, this behavior was not very clear in this study, probably due to the elevated Th content that was assessed, higher than U. Nevertheless, Th higher concentration values, which are common in REE minerals (Shives, 2015), confirms the value of this methodology for REE exploration in this target area, and additionally, it is in line with the pXRF results.

Although weathering can be an important mechanism of concentration for REE (e. g. Liu, 2022), the stream sediment survey showed REE are very much spatially associated with the SNAC and do not exhibit evident dispersion patterns. Nevertheless, the W-E fault trends north from SNAC and NW-SE trends seem to be the more promising areas for REE concentration in weather resistant minerals. Clearly, the weathering occurring around the Nejoio area is more noticeable due to the high concentrations in the source rocks, as shown from measurements.

Nb is enriched in the ijolites and alkaline dike swarms (NE-SW trend), to the south of the SNAC. However, samples with high concentrations of Nb (or Sn, W, Ta) may yield inaccuracies in pXRF when using pre-installed calibration (Somarin et al., 2021), and these results must be interpreted with reservations. Nevertheless, high measured concentrations seem to display this pattern, followed by phonolites, tinguaites and trachytes.

The wide distribution of K in stream sediments is expected, since K is present in unaltered SNAC lithologies, as well as granitic host rocks, but it also tends to be present in clays and alteration products from weathering. Alkaline igneous rocks are enriched in alkalis and so contain abundant Na and K-bearing minerals (such as feldspathoids). Likewise, K-feldspar is invariably present in the granites and granodiorites that form the host environment.

6. Conclusions

The spatial distribution of both radioelements, U and Th and the chosen set of elements measured by pXRF display a general view of the distribution of REE (Nb-Ta), which were the target materials in this work area, although data obtained by pXRF should be carefully interpreted, mainly due to the limitation regarding detection limits.

This work is a first step into understanding where the REE (and concurrently K and Th) are located within the SNAC to help understand the processes responsible for LREE and HREE concentration. REE concentrations are dominated by the Nejoio body, mainly due to one rock outcrop, that is probably affecting the stream sediment samples nearby, with very elevated Th and REE values. Syenites and ijolites are responsible for the higher concentrations in REE the SNAC. Nb is mainly associated with ijolites and phonolitic, tinguaitic and trachytic dikes. The surrounding rocks show little contribution for REE (Nb-Ta) concentration with the exception of aforementioned alkaline dikes rich in Nb that crosscut the area, mainly in a NE-SW trend.

The use of pGRS for mapping and exploration of alkaline environments was shown useful and more so the association of these two field techniques. K is ubiquitous in almost all lithological contexts of the study area. Even though U is more prone to mobilization in the surface environment and Th tends to stay immobile, in this region, this pattern was not clear. Th is present in larger quantities than U and the elevated concentrations in preferential directions in this complex is worth being investigated.

The lithological units present in SNAC are prone to anomalous concentrations of REE, phosphates, Ti, Zr, Ta, Nb, U and Th bearing minerals, yet mineralogical studies would be the next step to further understand this context.

Acknowledgments

The authors would like to thank Ivan Cuervo and the staff of the Instituto Geológico de Angola (IGEO) and UTE for all the support on the pursuit of the PLANAGEO work.

Authorship contribution statement

C. Prazeres: Writing - Original Draft, Conceptualization, Investigation, Visualization
M. J. Batista: Data Curation, Methodology, Investigation, Validation, Supervision, Formal analysis
R. Lopes: Investigation, Visualization, Review & Editing
B. Barros: Investigation, Visualization
J. Labaredas: Investigation, Visualization
J. F. Rodrigues: Project administration, Funding acquisition, Review & Editing
D. Cordeiro: Investigation, Resources

References

Banks, G., Walter, B., Marks, M., and Siegfried, P., 2019. A Workflow to Define, Map and Name a Carbonatite- or Alkaline Igneous-Associated REE-HFSE Mineral System: A Case Study from SW Germany. Minerals, 9 (2), 97; https://doi.org/10.3390/min9020097

Bau, M., and Dulsky, P., 1996. Distribution of yttrium and rare-earth elements in the Penge and Kuruman iron-formations, Transvaal Supergroup, South Africa. Precambrian Res., 79 (1996), pp. 37-55. DOI:0301-9268(95)00087-9

Borst, A., Finch, A., Nielson, G., Siegfried, P., Lopes, E., Eugenio, A., and Bambi, A. 2021 Alkaline magmatism and critical metals in Angola: Field observations and petrography of the Nejoio nepheline syenite complex. 7th International Geologica Belgica Meeting - Conference paper.

Chakhmouradian, A., and Wall, F., 2012. Rare Earth Elements: Minerals, Mines, Magnets (and More). Rare Earth Elements, Thematic Articles. Elements Magazine, October 2012.

Comin-Chiaramonti, P., Barros Gomes, C., Cundari, Al., Castorina, F., and Censi, P., 2007. A review of carbonatitic magmatism in the Paraná-Angola-Namibia (PAN) system. Periodico di Mineralogia 76 (2-3), 25-78 DOI:10.2451/2007PM0016.

Dostal, J., 2017. Rare element deposits of alkaline igneous rocks. Resources, 6, 34. DOI:10.3390/resources6030034

Fisher, L., Gazley, M., Baensch, A., Barnes, J., Cleverley, J., and Duclaux, G., 2014. Resolution of geochemical and lithostratigraphic complexity: a workflow for application of portable X-ray fluorescence to mineral exploration. Geochemistry: Exploration, Environment, Analysis. http://dx.doi.org/10.1144/geochem2012-158

IAEA, 2003. Guidelines for radioelement mapping using gamma ray spectrometry. IAEA TECDOD 1363.

Liu, W., Li, Y., Wang, X., Cui, L., Zhao, Z., Liu, C., and Xu, Z., 2022. Weathering stage and topographic control on rare earth element (REE) behavior: New constraints from a deeply weathered granite hill, Chemical Geology, Volume 610, 121066,ISSN 0009-2541, https://doi.org/10.1016/j.chemgeo.2022.121066.

Lopes, R., and Caessa, P, 2021. Geological Map of Angola 1:100 000, Sheet 295 – Capira and Sheet Report (1st edition). UTE (IGME, LNEG, Impulso) – IGEO, Luanda, 194p (in Portuguese).

Moyen, J-F., Cuney, M., Baratoux, D., Sardini, P., and Carrouée, S., 2021. Multi-scale spatial distribution of K, Th and U in an Archaean potassic granite: a case study from the Heerenveen batholith, Barberton Granite-Greenstone Terrain, South Africa. South African Journal of Geology, Vol 124. DOI:10.25131/sajg.124.0005

Murakami, T., Ohnuki, T., Isobe, H., and Sato, T. 1997. Mobility of uranium during weathering. American Mineralogist 82 (9-10): 888–899 https://doi.org/10.2138/am-1997-9-1006

Pereira, E, and Moreira, A., 1978. Sobre o complexo de estruturas anelares da Serra da Neve (Angola). II Centenário Academia das Ciências, Lisboa. Estudos de Geologia, Paleontologia e Micologia, 97-120 (in Portuguese).

Prazeres, C., Batista, M. J., Lopes, R., Barros, B., Labaredas, J., Silva T. P., Albardeiro, L., and Plastov J. M,. 2023. Rare Earth Elements potential in the Serra da Neve Calc-alkaline Complex, SW Angola – a first approach. Colloquium of African Geology - Windhoek, Namibia. Book of Abstracts.

Ravansari, R., Wilson, S., and Tighe, M, 2019. Portable X-ray fluorescence for environmental assessment

Rodrigues, B., 1972. Conclusions on the distribution of alkaline and carbonatitic complexes of Angola and Brazil. Revista da Faculdade de Ciências, vol XVII-Fasc1°, 2ªsérie, Ciências Naturais, 89-108.

Rodrigues, B., 1973. Processos de fenitização relacionados com a estrutura anelar do Nejoio. PhD thesis, University of Luanda, Angola, 308p (in Portuguese).

Somarin, A., Zhou, L., and Steinhage, I., 2021. Application of handheld XRF on Ta-Nb-Sn-W ore: Factory calibration or user calibration? Geochemical Journal, Vol. 55, pp. 149-158. DOI:10.2343/geochemj.2.0624

Shives, R., 2015. Using gamma ray spectrometry to find rare metals. In: Simandl, G. J. and Neetz, M. (Eds.). Symposium on strategic and critical materials proceedings, November 13-14, 2015, Victoria, British Columbia. British Columbia Geological